WELDING TECHNOLOGY R&D of JAPANESE ACCIDENT TOLERANT FeCrAl-ODS FUEL CLADDINGS FOR BWRs (2)

A. KIMURA, S. YUZAWA, Y. YAMASAKI, K. YABUUCHI
Institute of Advanced Energy, Kyoto University
Gokasho, Uji, Kyoto 611-0011, Japan

K. SAKAMOTO
Nippon Nuclear Fuel Development, Co., Ltd.
2163 Narita-cho, Oarai-machi, Ibaraki 311-1313, Japan

S. UKAI
Materials Science and Engineering, Faculty of Engineering, Hokkaido University
N13, W-8, Kita-ku, Sapporo 060-8628, Japan

A. YAMAJI
Waseda University
3-4-1, Okubo, Shinjuku-Ku, Tokyo 169-8555, Japan

K. KUSAGAYA
Global Nuclear Fuel – Japan, Co., Ltd.
3-1, Uchikawa 2-Chome, Yokosuka-Shi, Kanagawa 239-0836, Japan

T. KONDO
Hitachi-GE Nuclear Energy, Co., Ltd.
1-1, Saiwai-cho, 3-chome, Hitachi-shi, Ibaraki 317-0073, Japan

S. YAMASHITA
Japan Atomic Energy Agency
2-4 Shirakata Shirane, Tokai-mura, Naka-gun, Ibaraki 319-1195, Japan

ABSTRACT

The bond strength of end-capped cladding fabricated by electron beam (EB) welding method was measured to be in the range from 360 to 730 MPa, depending on the endcap material, wall thickness of cladding and applied voltage. The maximum bond strength was obtained for coupling of SUS430 endcaps and FeCrAl-ODS steel cladding, where the wall thickness at the weld bond was increased by the welding, although weld defects larger than 0.03 mm existed. X-ray CT revealed that the EB welding with the applied voltage of 150 kV caused the formation of weld defects as large as 0.1 mm, while at 60 kV no defect larger than 30μm was detected. The bond strength of the end-capped cladding with the weld defects larger than 30μm was at least 400 MPa. It is considered that a build-up welding is suitable for the endcap welding to cladding tube. The bond strength measurements after pressurized resistance welding (PRW) suggest that the weldability is degraded in the FeCrAl-ODS steels with higher Al content.

1. Introduction

FeCrAl-ODS steel is a promising candidate alloy for the accident tolerant fuel (ATF) cladding of light water reactors (LWRs) and being developed in Japanese projects recently [1,2]. This paper will show the current status of welding technology R&D of accident tolerant FeCrAl-ODS fuel claddings of boiling water reactors (BWRs) in the program sponsored and organized by the Ministry of Economy, Trade and Industry (METI) of Japan. This program is

being carried out to create the technical basis for the practical use of the ATF and the other components in LWRs through multifaceted activities. Both the experimental and the analytical studies have been performed in this program for R&D of FeCrAl-ODS fuel claddings [3].
High performance Al-added ODS steels for application to fast reactors have been successfully developed [4-6], and a number of researches including corrosion resistance [7,8], stress corrosion clacking [9], irradiation effects [10,11], hydrogen effects [12], aging effects [13], high reslution-TEM studies [14,15] were done so far.
Welding technology R&D is essential for application of ODS steel as an ATF cladding material of LWRs. ODS steels require special welding methods which never involve melting process because melting results in the agglomeration of oxide particles and consequently loss of the high performance of the steels such as high strength and radiation tolerance. It has been considered that solid state diffusion bonding [16,17] and friction stir welding (FSW) [18,19] are candidates for welding ODS steels. As for pressurized resistance welding (PRW), the previous research reported that endcap welding was done successfully for Al-free ODS steels [20,21]. Our recent study, however, showed the addition of Al often degraded weldability of ODS steels.
In the last meeting in Korea, we showed an example of successful work of conventional electron beam (EB) welding of FeCrAl-ODS cladding and SUS430 endcaps. Furthermore, we also reported that endcup welding was easy for Al-free ODS steels but the addition of Al often degraded weldability of ODS steels.
In this research, the EB welding conditions are explored for welding endcaps to FeCrAl-ODS steel cladding with focusing on the effect of Al content in the materials. The bond strength is measured for the endcap welded cladding tube, and non-destructive inspections are applied to detect welding defects. Pressurized resistivity welding is also performed for FeCrAl-ODS steels with different Al content.

2. Experimental

2.1 Materials

The materials used in this research are FeCrAl-ODS steels (15Cr4Al-ODSS(KNOP5) and 12Cr6Al-ODSS) and ferritic steels (SUS430 and 12Cr6Al steel) of which the chemical compositions are shown in Table 1. The ODS steels were produced by mechanical alloying for 48 hr starting with each elemental metal powders. The mixed powder was encapsulated into a steel capsule and extruded at 1150ºC. The pilger-rolled tubing was carried out to produce cladding tubes with 8.5 mm outer diameter, 0.5 mm thickness and 1200 mm length for 15Cr4Al-ODSS and 11.15 mm outer diameter, 0.3 mm thickness and 1200 mm length for 12Cr6Al-ODSS. The final heat treatment conditions of the ODS steels are annealing at 1150ºC for 1 hour in air followed by air cooling. An ingot (19 kg) of FeCrAl ferritic steel was produced by vacuum melting method and forged into rods with 22 mm diameter at 1200 ºC. The endcaps were produced from the rods.
The sheet type FeCrAl-ODS steel specimens for PRW are in as-extruded condition, in which the grains were elongated along the extrusion direction with the grain length of less than 1 μm and width of 0.3 μm. In contrast, the FeCrAl-ODS steel tube has rather coarse grains because of cyclic recrystallization process including cold works and annealings, being several hundreds μm length and several tens μm width.

	C	Si	Mn	P	S	Cr	W	Al	Ti	Y	O	N	Ar	Zr	Y_2O_3	Ex.O
SUS430	0.018	0.15	0.74	-	-	16.00	-	-	-	-	-	-	-	-	-	-
KNOP5	0.031	0.03	0.02	<0.005	0.002	15.15	1.9	3.9	0.11	0.26	0.14	0.005	0.005	0.58	0.33	0.07
FeCrAl	0.002	0.04	0.05	<0.005	0.001	12.0	<0.005	6.1	0.51	-	0.004	0.003	<0.001	0.47	-	-
FeCrAl-ODS	0.025	0.02	0.02	<0.005	0.003	11.6	<0.01	6.15	0.49	0.38	0.34	0.01	0.005	0.39	0.48	0.24

Tab 1: Chemical compositions of the steels used for EB welding of endcap (SUS430, 12Cr6Al steel) and tube (15Cr4Al-ODS steel, 12Cr6Al-ODS steel).

2.2 Welding method and conditions

EB welding was subjected for the endcaps made of SUS430 to a tube made of FeCrAl-ODS steel, of which the welding conditions were shown in Tab 2. PRW was carried out for three sorts of ODS steels with different content of Al. The welded specimen geometry measures 6 mm width, 40 mm length and 0.6 mm thickness. Overlapping welding was performed for two sheet types of ODS steels. The load for pressing is 500 N and the electric power was set at 6 kW for FeCrAl-ODS steel specimen. The detailed welding conditions were shown in Tab 2.

(a) PRW	
Materials	FeCrAl-ODS
Load [N]	500
Power [W]	6,000
Voltage [V]	1.541
Current [A]	3,941
Resistivity [mΩ]	0.39

(b) EB	
Endcap/SUS430 Tube/FeCrAl-ODS	
Fusion [mm]	0.48, 0.79,1
Voltage [kV]	60,150
Current [A]	2,3,4
Scan [m/min]	1

Tab 2: (a) PRW and (b) EB welding conditions.

2.3 X-ray CT and UT detection

X-ray computed tomography (CT) is a nondestructive technique for visualizing interior features within solid objects, and for obtaining digital information on their 3-D geometries and properties. X-ray CT inspection can provide the defects of complex weld bond by looking into the internal structure. The CT capability is used to qualify and quantify damage structures such as voids and cracks inner or outer dimension in a smooth, non-destructive process. The X ray CT conditions are shown in Tab 3.

Items	Conditions	Items	Conditions
Source Voltage [kV]	225	Field Size	9.0
Tube Voltage [kV]	200	Magnification	22.2
Sensor	Flat Panel	Pixel Size [mm]	0.00917
SID [mm]	500	Projection/Average	3,000/1
SOD [mm]	22.5	Reset Time [msec]	1000
CT mode	Centered	Exposure Time [hh:mm]	00:50

Tab 3: X ray-CT conditions

Ultrasonic flow detection method was applied to detect welding defects like pores at the joint. As the tube thickness was 0.3 mm, the detection limit was required to be 0.1 mm at least. Water immersion vertical flaw method, which can select a few inspection refraction angles and the degree of diffusion of an ultrasonic beam, was adopted. The inspection conditions are shown in Tab 4.

Items	Conditions
Probe	20 MHz
	Φ 0.25 inch, PF=0.75inch
Gate [mm]	0.6 – 2.9
Distance [mm]	15
Speed [m/s]	5790

Tab 4**:** Water immersion vertical flaw method

2.4 Tensile test and microstructural examination

Tensile tests were carried out for endcap-welded tube samples at room temperature at the displacement rate of 0.5 mm/min with use of an Instron test machine. After tensile tests, fracture surface was observed by scanning electron microscope (SEM). The cross sectional views of weld bonds were observed after the tensile tests. The tensile tested samples were cut into two pieces along axis direction and the cut surface of the weld bond was mechanically polished with SiC papers from #500 to #2000 and finally buff-polished with the diamond past with the diameters from 3 to 0.25 μm.

3. Experimental Results

3.1 Electron beam (EB) welding

3.1.1 Tensile test

The appearance of the endcap welded tube samples is shown in Fig. 1. For tensile tests, a pin hole was produced in the endcap and tested at room temperature. The stress strain curves of the endcap welded tube samples were shown in Fig. 2. As shown in the stress-strain behavior, all the samples broke without plastic deformation at the joint of the endcap and FeCrAl-ODS steel tube. The fracture stress is ranging from 350 to 660 MPa, although most of them were around 450 MPa. The fracture mode was a mixed mode of ductile and quasi cleavage. The previous tensile test results showed that the EB welded SUS430 endcap and 15Cr4Al-ODS steel clad tube broke in the ODS steel tube far from the weld bond after enough amount of plastic deformation. The fracture stress was 730 MPa and tensile strain is larger than 6 %. The fracture mode was completely ductile. This trend is very different from present results. It is considered that the difference in the strength of the weld joint is due to the difference in the Al content of both the materials of endcap and clad tube. In the previous rests, the endcap was made of SUS430 that contained no Al and the amount of Al in the ODS steel clad tube was 4wt.%. As we reported in the previous paper, Al has a detrimental effect on the weldability. It is notable that the specimen surface of Al-added ODS steel is often covered by thin alumina [7, 8] layer, which is formed spontaneously during production of the specimens, and has a much higher electric resistivity and causes much larger Joule heating. Especially, in the case of resistivity welding of Al-added ODS steel, it is recommended that the surface thin alumina layer should be removed just before the welding. The effect of surface polishing on the weldability of Al-added ODS steel will be shown in the meeting (WRFPM2018).

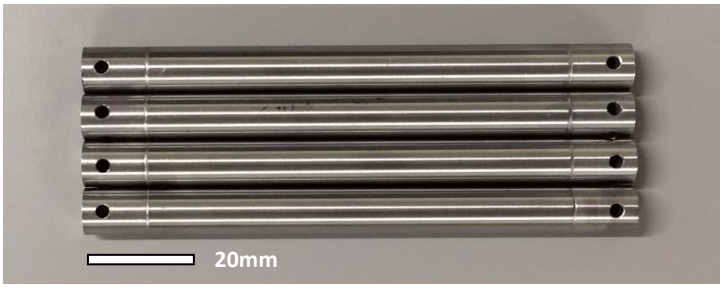

Fig 1. Tensile specimens with EB welded endcaps at both sides.

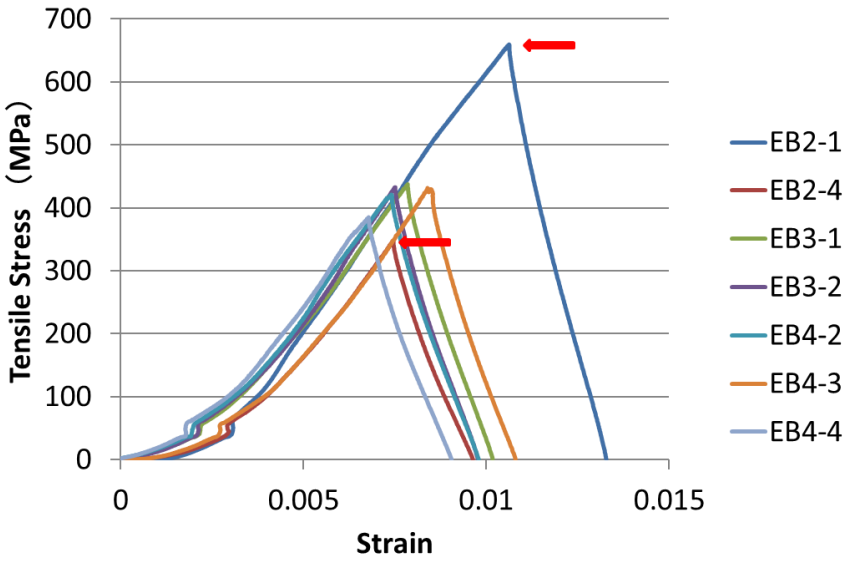

Fig 2. Stress-strain behavior of EB welded tensile specimen shown in Fig. 1.

3.1.2 Fracture behavior

Fracture mode of the tensile tested specimens is shown in Fig. 3. Fig.3(a) shows a mixed mode of ductile and quasi cleavage mode of which the fracture stress was the largest; 659 MPa. Fig.3(b) shows a large pore on the fracture surface and the fracture stress was 450 MPa. Fig.3(c) shows the fracture surface with smallest bond strength among the tested specimens in which the bonded part got thin after EB welding. Most of the fracture modes were brittle in all the three cases as shown in Fig. 3. Since the tensile test temperature was RT and usually the materials were ductile at RT before welding, it can be said that the joint portion was embrittled by EB welding. Post-weld heat treatment might be necessary to overcome the welding induced embrittlement. It should be noted that no larger pore than 100 μm was observed on the fracture surfaces in the specimens of which the fracture stresses were maximum (a) and minimum (c). However, as shown in Fig. 3(b), the specimen with 450 MPa of fracture stress clearly shows a large pore (100 μm), indicating that the weld pores are not always the cause of the reduction of fracture stress. The bottom of Fig. 3(c) indicates that the weld line portion got thin after EB welding as mentioned before. The reduction of thickness results in the increase in the stress applied, and fracture occurred at the joint portion.

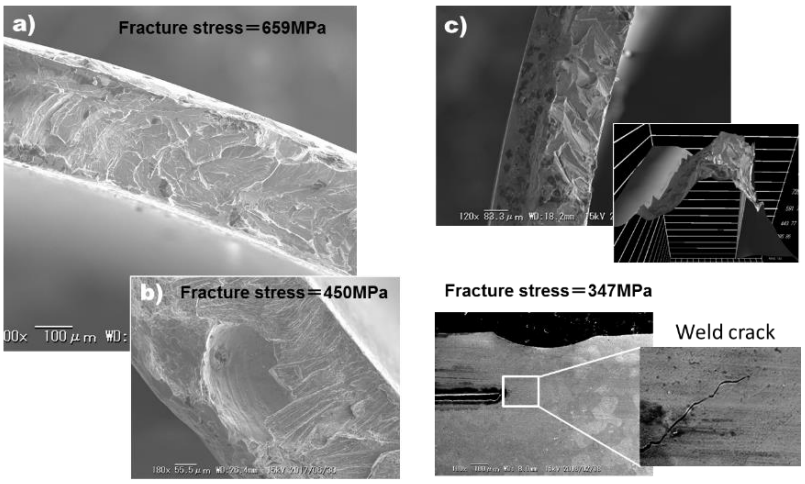

Fig 3. Fracture mode of the tensile tested specimens: a) a mixed mode of ductile and quasi cleavage mode of which the fracture stress was the largest; 659 MPa, b) a large pore was observed on the fracture surface: fracture stress was 450 MPa, c) The fracture stress was smallest (347 MPa) among the tested specimens. The bonded part got thin.

3.1.3 X ray-CT inspection

Before tensile test, X ray-CT was carried out for both endcaps of EB welded samples, and results are shown in Fig. 4. Fig.4(a) is one of the planes of radial cross section views of the endcap welded tube with the maximum fracture stress, and Fig. 4(b) is that of the minimum fracture stress. The 3-dimentional view of X ray-CT is also shown which clearly show that there is almost no pore visible by this inspection. This is due to setting a low beam current of EB welding. It is noticed that there is a depletion at the joint especially in Fig. 4(b) of which the fracture stress was a minimum. As mentioned in the previous session, this depletion is the cause of the minimum fracture stress.

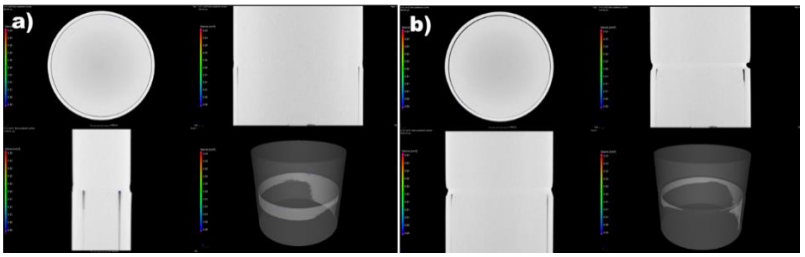

Fig 4. Examples of X-ray CT inspection: The fracture stress is a) 659 MPa and b) 347 MPa.

3.1.4 UT detection

Water immersion vertical flaw method is suitable to detect voids or pores formed by welding and applied for the EB welding joint. It was recognized that there is a dead zone of 0.6 mm length from the endcap bottom caused by surface echo. The surface roughness also increases the dead zone length and invades to detection gate, which is enhanced in the vacant area between the endcap and tube. It is considered that UT is not adequate for the detection of pores with the size of 0.1 mm diameter, although there is a possibility to analyze the wave shape to distinguish the surface echo and tube bottom echo.

3.2 Pressurized resistivity welding (PRW)

3.2.1 Overlapping welding

T-bone type sheet specimens were fabricated from three sorts of FeCrAl-ODS steels (12Cr-5Al-ODSS, 15Cr-6.5Al-ODSS and 14Cr-8Al-ODSS). A pair of sheet specimens were overlapping-welded by pressurized resistivity welding method (Fig. 5). A special specimen holder was produced to keep an alignment of tensile specimens steady.

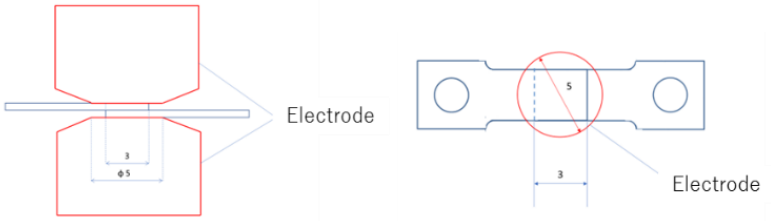

Fig 5. Specimens for PRW

3.2.2 Fracture load measurements

Fig. 6 shows the relationship between fracture load and current imposed by PRW. The materials contain different amount of Cr and Al. As already shown in the previous report on the effect of Al on the weldability, Al degraded it. Here, again, Fig. 6 indicates similar trends. There are three sorts of FeCrAl-ODS steels and each group of the results shows that with increasing the current the fracture load increases. However, in 14Cr-8Al ODS steel too high current causes the reduction of fracture load. This trend was also observed for the other two ODS steels, although all the data were not shown in the figure. It can be said that Al again degraded the weld bond strength. Since the main difference in the material compositions is Al among the three, it is suggested that the welding heat can be accumulated more in the Al-added ODS steel than the low-Al ODS steel because of the lower thermal conductivity, higher specific heat and larger electric resistivity of the steels with higher Al content.

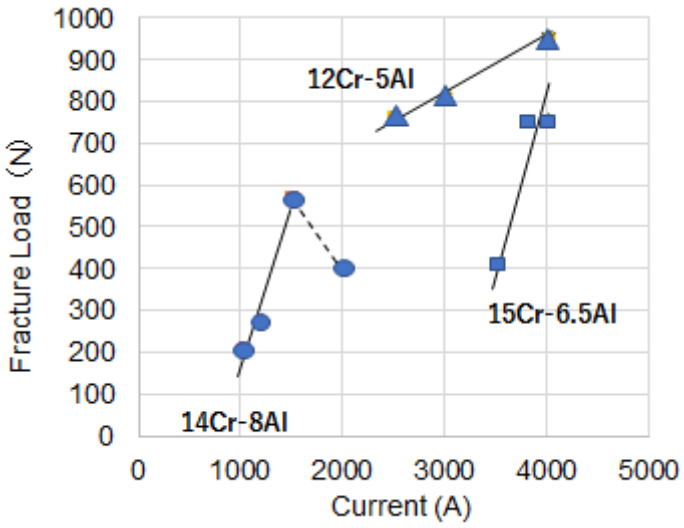

Fig 6. The relationship between fracture load and current imposed by PWR.

4. Assessment of Weldability

4.1 EB weld conditions

In this session the EB weldability is discussed based on the following EB welding results obtained so far. The previous results are summarized as following 3 cases.

Case 1: 15Cr-4Al-ODS cladding/SUS430 endcap, 150kV、2mA、0.5mmt
Case 2: 15Cr-4Al-ODS cladding/15Cr-4Al-ODS endcap, 150kV、2mA、0.5mmt
Case 3: 12Cr-6Al-ODS cladding/12Cr-6Al steel endcap, 60kV、2-4mA、0.35mmt

In Case 1, the fracture occurred in the cladding tube, which indicates the bonding strength is higher than that of cladding, namely, 730 MPa. The weld bond microstructure was sound showing no pore larger than 50 μm. The fusion depth of the bond area was about 1 mm that is thick enough for the cladding tube thickness of 0.5 mm. There was no clacking induced by welding. It should be noticed that the wall thickness of fusion region was increased in this case, which resulted in the decrease in the stress at the bond. This explains why the fracture occurs in ODS steel cladding not at the weld bond made of SUS430 steel with much lower strength than ODS steel.

In Case 2, the available weld bond strength was 450 MPa which was still large enough for the requirement of cladding tube strength with the consideration of aseismatic performance as shown latter. X-ray-CT inspection clearly indicated the presence of pores which were the cause of the bonding strength. The comparison of Case 1 and 2 suggests that Al in the endcap degrades weldability. It is considered that the alumina spontaneously formed on the specimen surface increased the resistivity and resultantly Joule heating, which resulted in the formation of rather large pores.

Case 3 is the most suitable coupling for practical application. In this research, the bond strength was ranging from 360 to 660 MPa. The X-ray CT inspection results showed that there was no larger pores than 30 μm, while the wall thickness of the bond region was thinner than 0.3 mm. This is the reverse situation to Case 1 where the wall thickness was thicker than 0.35 mm. No pore formation here is due to a low voltage application, that is, 60 kV not 150kV. So it is expected that the Case 3 with a bit higher applied voltage, like 80 to 100 kV, offers good weld bond with no pores and enough wall thickness. By consequence, it is strongly recommended that build-up welding is suitable for the end-cap welding to cladding tube.

4.2 Aseismatic Performance Evaluation

Based on the seismic intensity method, aseismatic performance was evaluated, where the maximum horizontal acceleration is 0.46 G (450 gal) for nuclear reactor. The seismic load applied to the cladding tube is calculated to be 391 N and the converted value to the shear stress at the bonding is 32 MPa. More serious condition is the hoop stress induced by fission products, which is estimated to be 110 MPa at the end of the lifetime of cladding. The long term allowable stress for seismic resistance is defined to be 2/3 of the yield stress of the steel components, while the short term allowable stress is the yield stress of the steel. Since the yield stress of the EB welded samples is at least 360 MPa, the long term allowable stress is calculated to be 240 MPa that is high enough for the requirement of cladding tube strength of 110 MPa.

5. Conclusion

In this research, the EB welding conditions are explored for welding endcaps and FeCrAl-ODS steel clad with focusing on the effect of Al content in the materials. The bond strength is measured for the endcap welded cladding tube and non-destructive inspections are applied to detect weld defects. Pressurized resistivity welding is also performed for FeCrAl-ODS steels with different Al content. The obtained main results are as follows:

1) The bond strength of end-capped cladding fabricated by EB welding method was measured to be in the range from 360 to 730 MPa, depending on the endcap material, wall thickness of clads, applied voltage. The maximum bond strength was obtained for coupling of SUS430 endcaps and 15Cr4Al-ODS steel cladding, where the wall thickness at the weld bond was

increased by the welding, although weld defects larger than 0.03 mm existed.
2) X-ray CT inspection revealed that the EB welding with the applied voltage of 150 kV caused the formation of weld defects as large as 0.1 mm, while at 60 kV no defect larger than 0.03 mm was detected. The bond strength of the end-capped cladding with the weld defects larger than 0.03 mm was around 450 MPa.
3) It is considered that build-up welding is suitable for the end-cap welding to cladding tube.
4) The bond strength measurements after PRW suggest that the weldability was degraded for the FeCrAl-ODS steels with high Al content.

Acknowledgement

A part of this study is the result of “Development of Technical Basis for Introducing Advanced Fuels Contributing to Safety Improvement of Current Light Water Reactors” carried out under the Project on Development of Technical Basis for Improving Nuclear Safety by Ministry of Economy, Trade and Industry (METI) of Japan.

References

[1] S. Ukai, N. Oono, S. Ohtsuka, T. Kaito, K. Sakamoto, T. Torimaru, A. Kimura, S. Hayashi, "Development of FeCrAl-ODS steels for ATF cladding", Proceedings of Top Fuel 2016, Boise, ID, Sep. 11-15 (2016) 681-689.
[2] K. Sakamoto, M. Hirai, S. Ukai, A. Kimura, A. Yamaji, K. Kusagaya, T. Kondo, S. Yamashita, "Overview of Japanese development of accident tolerant FeCrAl-ODS fuel claddings for BWRs", Proceedings of 2017 Water Reactor Fuel Performance Meeting, Ramada Plaza Jeju, Jeju Island, Korea, Sep. 10-14 (2017) Paper ID: A-033.
[3] A. Kimura, T. Takayama, P. Song, W. Han, K. Yabuuchi, P. Dou, “Dispersion Control of Oxide Particles in FeCrAl-ODS Ferritic Steels for Application to ATF Cladding”, FiMPART-2017, (2017).
[4] A. Kimura, S. Ukai, M. Fujiwara, “Development of fuel clad materials for high burn-up operation of LWR”, Proc. of GENES4/ANP2003, ISBN: 4-901332-01-5, CD-ROM file (2003) 1198.
[5] A. Kimura, H.S. Cho, N. Toda, R. Kasada, K. Yutani, H. Kishimoto, N. Iwata, S. Ukai and M. Fujiwara, “High Burnup Fuel Cladding Materials R&D for Advanced Nuclear Systems－Nano-sized Oxide Dispersion Strengthening Steels”, J. Nucl. Sci. Technol. 44(3) (2007) 323-328.
[6] A. Kimura, R. Kasada, N. Iwata, H. Kishimoto, C.H. Zhang, J. Isselin, P. Dou, J.H. Lee, N. Muthukumar, T. Okuda, M. Inoue, S. Ukai, S. Ohnuki, T. Fujisawa, F. Abe, “Development of Al added high-Cr ODS steels for fuel cladding of next generation nuclear systems”, J. Nucl. Mater. 417 (2011.10.01) 176-179.
[7] J. Isselin, R. Kasada, a. Kimura, “Corrosion behavior of 16%Cr–4%Al and 16%Cr ODS ferritic steels under different metallurgical conditions in a supercritical water environment”, Corrosion Science, 52 (2010) 3266–3270.
[8] H.S. Cho, A. Kimura, S. Ukai and M. Fujiwara, “Corrosion Properties of Oxide Dispersion Strengthened Steels in Super-Critical Water Environment”, J. Nucl. Mater. 329-333 (2004) 387-391.
[9] H.I Je, A. Kimura, “Stress corrosion cracking susceptibility of oxide dispersion strengthened ferritic steel in supercritical pressurized water dissolved with different hydrogen and oxygen contents”, Corrosion Science 78 (2014.01) 193-199.
[10] T. Yoshitake, Y. Abe, N. Akasaka, S. Ohtsuka, S. Ukai and A. Kimura, “Ring-Tensile Properties of Irradiated Oxide Dispersion Strengthened Ferritic/Martensitic Steel Claddings”, J. Nucl. Mater. 329-333 (2004) 342-346.
[11] K. Yutani, H. Kishimoto, R. Kasada and A. Kimura, “Evaluation of Helium effects on Swelling Behavior of Oxide Dispersion Strengthened Ferritic Steels under Ion Irradiation”, J. Nucl. Mater. 367-370 (2007) 423-427.
[12] J.S. Lee, A. Kimura, S. Ukai and M. Fujiwara, “Effects of Hydrogen on the

Mechanical Properties of Oxide Dispersion Strengthening Steels", J. Nucl. Mater. 329-333 (2004) 1122-1126.
[13] J.S. Lee, C.H. Jang, I.S. Kim and A. Kimura, "Embrittlement and Hardening during Thermal Aging of High Cr Oxide Dispersion Strengthened Alloys", J. Nucl. Mater. 367-370 (2007) 229-233.
[14] P. Dou, A. Kimura, T. Okuda, M. Inoue, S. Ukai, S. Ohnuki, T. Fujisawa, F. Abe, "Polymorphic and coherency transition of Y–Al complex oxide particles with extrusion temperature in an Al-alloyed high-Cr oxide dispersion strengthened ferritic steel", Acta Materialia 59 (2011) 992-1002.
[15] P. Dou, A. Kimura, R. Kasada, T.Okuda, M. Inoue, S. Ukai, S. Ohnuki, T. Fujisawa, F. Abe, "Effects of titanium concentration and tungsten addition on the nano-mesoscopic structure of high-Cr oxide dispersion strengthened (ODS) ferritic steels", J. Nucl. Mater. 442 (2013.11) S95-S100.
[16] S. Noh, R. Kasada, A. Kimura, "Solid-state diffusion bonding of high-Cr ODS ferritic steel", Acta Materialia 59(8) (2011.05) 3196-3204.
[17] S. Noh, B.J. Kim, R. Kasada, A. Kimura, "Diffusion bonding between ODS ferritic steel and F82H steel for fusion applications", J. Nucl. Mater. 426(1-3) (2012.03.05) 208-213.
[18] W. Han, a. Kimura, D. Chen, Z. Zhang, H. Serizawa, Y. Morisada and H. Fujii, "Parameter Selection in Dissimilar Friction Stir Welding of ODS Ferritic Steel and RAFM Steel F82H", J. Plasma Fusion Res. SERIES 11 (2015.3.30) 65-68.
[19] W. Han, D. Chen, Y.S. HA, A. Kimura, H. Serizawa, H. Fujii, Y. Morisada, "Modifications of grain-boundary structure by friction stir welding in the joint of nano-structured oxide dispersion strengthened ferritic steel and reduced activation martensitic steel", Scripta Materialia, 105 (2015.08) 2-5.
[20] J. Bottcher, S. Ukai, M. Inoue, "ODS steel clad mox fuel-pin fabrication and irradiation performance in EBR-II", J. Nucl. Technol., 138 (2002), 238
[21] S. Ukai, M. Fujiwara, "Perspective of ODS alloys application in nuclear environments", J. of Nucl. Mater., 307–311, Part 1, 749–757.